Journal of Sustainable Development of Energy, Water and Environment Systems

http://www.sdewes.org/jsdewes

Year 2026, Volume 14, Issue 2, 1140667

Original Research Article

Impact of Electric Vehicle Charging on the Distribution Network of Oujda City, Morocco

***Mouad Karmoun*[*1], *Wafae Arfaoui*[1], *Smail Zouggar*[1], *Mohamed Laarbi Elhafyani*[1], *Hassan Zahboune*[1], *Taoufik Ouchbel*[1], *Adrian Alarcon Becerra*[2], *Nikola Matak*[3]**

[1]University Mohammed 1, School of Technology, Laboratory of Electrical Engineering and Maintenance (LEEM). BP, 473, 60000 Oujda. Morocco

[2]CIRCE Dinamiza Business Park Ranillas Avenue Building 3D, 1er étage 50018, Saragosse España

[3]University of Zagreb, Faculty of Mechanical Engineering and Naval Architecture, Ivana Lucica 5, 10000 Zagreb, Croatia

e-mail: mourad.karmoun@ump.ac.ma, arfaouiwafae2@gmail.com, smail.zouggar@ump.ac.ma, m.elhafyani@ump.ac.ma, H.zahboune@ump.ac.ma, t.ouchbel@ump.ac.ma, acalarcon@fcirce.es, nikola.matak@fsb.unizg.hr

Cite as: Karmoun, M., Arfaoui, W., Zouggar, S., Zahboune, H., Elhafyani, M. L., Ouchbel, T., Matak, N., Becerra, A. A., Impact of Electric Vehicle Charging on the Medium Voltacge Network of Oujda, Morocco, J.sustain. dev. energy water environ. syst., 14(2), 1140667, 2026, DOI: https://doi.org/10.13044/j.sdewes.d14.0667

ABSTRACT

Electric-vehicle charging can erode operating margins in distribution networks, yet impacts are often localized rather than system-wide. This study quantifies unmanaged charging effects on the Oujda 60/22-kV system using a geo-referenced steady-state power-flow model coupled with a stochastic charging generator for cars, motorcycles and buses. The network representation comprises 124 substations and 117 branches, and we examine snapshots at 0%, 10% and 30% adoption. In thermal terms, the bulk of the network remains comfortably loaded: the share of lines operating at ≤70% of their rating is 81% at baseline, 79% at 10% and 78% at 30%. Localized constraints intensify modestly with penetration: the share of overloaded lines (>100%) rises from 6% to 7% and 9%, and the worst-loaded span increases from 151.6% to 157.2% and 168.1%. Voltage performance is similarly robust in bulk (median around 0.97 per unit), with a small weak-bus tail near charging hotspots. All cases converged reliably. The workflow is lightweight and reproducible, supporting feeder-level hosting-capacity screening and motivating targeted reinforcement or simple smart-charging measures in data-constrained systems.

KEYWORDS

Energy transition, Electric vehicle integration, Stochastic modeling, Load profiling, Urban power grids, Gridcal.

INTRODUCTION

Electric vehicles (EVs) are being integrated into urban power grids, creating both opportunities and challenges for system operation. As adoption accelerates driven by environmental goals and policy incentives assessing the impacts of EV charging on grid performance is critical for reliability and efficiency. According to the International Energy

* Corresponding author

Agency, the global stock of electric cars surpassed 10 million in 2020, a 43% increase over 2019 despite the COVID-19 downturn [1], and continued growth is expected as transport decarbonizes.

Shifting focus to a regional perspective, Morocco has emerged as a leader in sustainable development, targeting 96% renewable electricity generation by 2050 through aggressive investments in solar, wind, and hydropower. This transition is critical for decarbonizing key sectors, particularly transportation, which accounts for 27% of national greenhouse gas emissions [2]. Morocco's Nationally Determined Contribution under the Paris Agreement highlights renewable energy integration and EV adoption as pivotal strategies to meet its environmental objectives [3]. Moreover, the nation’s ambition to become a manufacturing hub for EV batteries and components is underscored by plans for a USD 2 billion gigafactory dedicated to lithium-ion battery production, supporting the annual manufacturing of 300,000 to 500,000 EVs. This strategy builds on Morocco’s robust automotive industry, which currently produces over 700,000 vehicles per year [4]. However, before such ambitions can be fully realized, it is necessary to comprehensively analyze the implications of large-scale EV adoption on the country's power grid infrastructure [5]

Recent Africa-focused evidence is emerging but remains sparse relative to Europe and East Asia. In Morocco, medium-voltage case studies report that integrating electric-vehicle chargers in urban feeders (Casablanca) increases evening peaks and aggravates localized undervoltage and harmonic exposure, underscoring the need for feeder-level siting and coordination [5]. For Sub-Saharan systems, a South African hosting-capacity study demonstrates that even single-phase charging can materially constrain low-voltage networks and illustrates a Monte-Carlo workflow designed for minimal data environments − directly relevant to Oujda’s planning context [6]. A recent regional review synthesizes deployment barriers (distribution readiness, charging siting, tariff design) and highlights the importance of lightweight, reproducible methods for utilities operating with limited telemetry [7]. These findings motivate our geo-referenced, data-efficient workflow and our focus on feeder-level loading bands and voltage-quality indicators.

Technically, rising EV adoption reshapes demand patterns on power grids, particularly at the distribution level, introducing significant operational challenges if charging remains unmanaged. Uncontrolled EV charging can increase peak loads, risking infrastructure overloads [8]. The spatial clustering of this demand can cause voltage deviations and power quality issues [9], while also creating the potential for voltage instability in weak-grid areas or at feeder extremities [10]. Aggregated charging loads may threaten the thermal limits of transformers and cables, potentially reducing asset lifespan [11]. In broader terms, Sarda *et al.* [12] review how these integration challenges impact overall system efficiency, while Sundstrom and Binding [13] specifically quantify the increase in distribution losses when grid constraints are not actively managed. Furthermore, the proliferation of high-power fast-charging stations may create harmonic distortions, further complicating power quality management [14]. These multiple, interrelated challenges underscore the need for detailed impact studies and effective grid enhancements.

To address these challenges, smart charging algorithms that coordinate charging rates and times have demonstrated effective peak-demand mitigation and load smoothing [15]. A more advanced bidirectional operation, Vehicle-to-Grid (V2G), has also been proposed. In V2G, aggregated EVs modulate charging and can export power to provide peak shaving, feeder-level voltage support, and ancillary services when coordinated with distribution constraints [16]. Recent studies have explored various aspects of Vehicle-to-Grid (V2G) integration. Sovacool *et*

al. [17] reviewed the business models and innovation systems required to facilitate V2G technology adoption. Kumar *et al.* [18] provided a comprehensive overview of V2G integration, emphasizing its potential to power future energy systems. Furthermore, Mastoi *et al.* [19] analyzed specific charging-dispatch strategies within distribution networks to optimize grid flexibility while managing constraints. Deep reinforcement learning has also been applied for optimal V2G frequency regulation [20]. In this paper, we quantify today's unidirectional (G2V) impacts for Oujda; V2G is scoped as future work to test feeder-level benefits in the 60/22 kV network.

In line with these operational concerns, accurate modeling of EV charging demand emerges as a critical component for evaluating its implications on the power grid. Various methodologies have been explored in the literature to address this challenge. Stochastic modeling, such as the Monte Carlo simulation framework developed by Richardson *et al.* [21], incorporates randomness in factors like arrival times, state-of-charge, and charging durations to capture real-world variability and assess demand scenarios with associated probabilities. Similarly, spatial distribution plays a significant role, with research by Mu *et al.* [22] highlighting how clustering of charging stations in specific areas can strain local networks, exacerbate voltage and loading issues. Together, these approaches contribute to a comprehensive understanding of EV charging demand dynamics and their broader impact on the power grid.

To further explore these dynamics, simulation tools play a vital role in assessing the effects of EV integration on power grids. Among commonly utilized software, GridCal stands out as an open-source tool supporting power flow calculations, time-series simulations, and hosting capacity assessments, with its Python compatibility enhancing flexibility for custom studies [23]. OpenDSS, developed by the Electric Power Research Institute (EPRI), provides a comprehensive framework for modeling electric power distribution systems, enabling advanced analyses such as harmonic studies and quasistatic time-series simulations [24]. Similarly, MATPOWER, a MATLAB-based package, is widely adopted in academia for its user-friendly design and its capability to perform power flow and optimal power flow analyses for both transmission and distribution networks [25]. These simulation tools collectively empower researchers to construct detailed power system models, simulate diverse conditions, and devise effective strategies to address emerging challenges related to EV integration.

Study Scope

We conduct a two-stage, steady-state assessment for Oujda City. In the first stage, a stochastic EV-charging model generates an 8,760-hour load profile customized to the city's vehicle fleet and seasonal usage patterns. In the second stage, the annual average power derived from this profile serves as the steady-state input for an alternating-current power-flow simulation using GridCal API. Voltage levels and line loading are analyzed under 0%, 10%, and 30% EV adoption scenarios to provide actionable insights for utility planners.

Key Contributions

This article offers three main contributions: (i) a city-level assessment that spatially allocates public EV charging to real candidate sites (i.e., gas stations), with load injections mapped to the nearest buses in a geo-referenced medium-voltage network model; (ii) a data-efficient and reproducible workflow that generates planner-relevant indicators – such as the proportion of grid elements within ≤70%, 70 – 90%, 90 – 100%, and >100% loading bands, as well as the number of buses operating below 0.95 per unit voltage under unmanaged charging scenarios; (iii) an evidence-based identification of grid "hotspots" in Oujda at 10% and 30% EV adoption levels, enabling feeder-level hosting capacity planning in data-constrained environments.

METHODS

This section describes a portable, city-scale workflow to assess unmanaged EV charging impacts. A stochastic charging generator is coupled to an alternating-current Newton–Raphson power-flow solver to produce feeder- and bus-level stress indicators for a single steady-state scenario.

Study Design and Workflow

The workflow proceeds in six steps (illustrated in **Figure 1**):

1. **Stochastic charging profile generation.** A full 8,760-hour, seasonal load profile is generated for each vehicle class (cars, motorcycles, and buses) as detailed in Stochastic charging model and assumptions.
2. **Average power calculation.** From the hourly profile, an annual average charging power (MW) is computed to represent the steady-state injection.
3. **Spatial allocation of charging.** Average EV power is partitioned and mapped to the network at **proposed public charging sites** (gas stations) and at home/work locations.
4. **Network coupling.** For each adoption scenario (0%, 10%, 30%), the bus-level average EV demand is **superposed** on the base (non-EV) load.
5. **Power-flow solution.** A single steady-state alternating-current Newton – Raphson solve provides bus voltages and branch flows.
6. **Stress quantification.** Thermal-loading bands and voltage-compliance metrics are computed (definitions in Line-loading definition and stress metrics).

Design priorities are portability (explicit inputs and tolerances), operator relevance (loading bands and voltage-band compliance), and transparency (tabular artefacts suitable for audit).

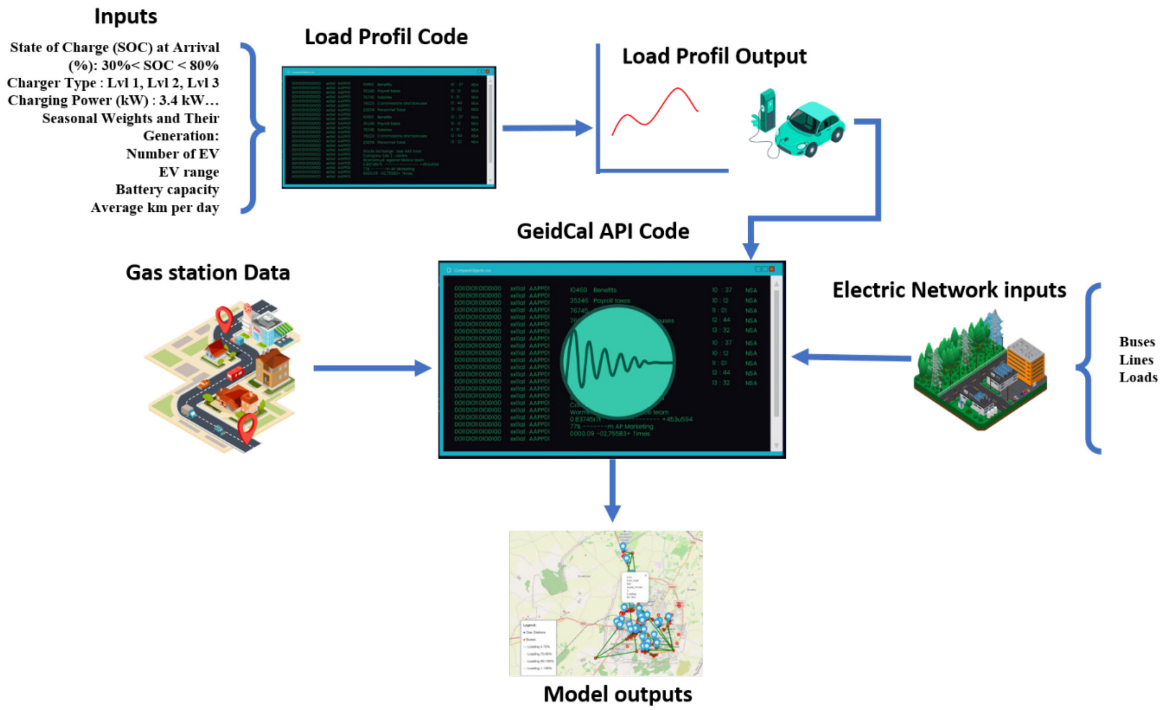

Figure 1.Overview of the approach

Data and Network Model

The Oujda distribution network is implemented in GridCal from operator spreadsheets (buses, lines/transformers, loads, and generators) with geospatial attributes and ratings (**Table 1**).

- **Buses:** identifier, nominal voltage (kV), latitude/longitude, voltage limits $[V_{\min}, V_{\max}]$, slack flag.
- **Branches (overhead/transformer):** series R, X, thermal rating S_{rate}(MVA), connectivity (from, to).
- **Loads:** connection bus, base active $P$and reactive Q.

Table 1. Summary of the Oujda medium-voltage network used in the power-flow analysis

Parameter	Value	Description
Network Model	Oujda MV Grid	Medium-voltage distribution network
Total Buses	124	Includes substations and load connection points
Total Lines	117	22 kV overhead lines and cables
Nominal Voltage	22 kV	Fed from 60 kV and 225 kV substations
System Base Power	400 MVA	Base value for per-unit calculations
Total Base Load (P)	177.01 MW	Total active power demand (non-EV)
Total Base Load (Q)	141.61 Mvar	Total reactive power demand (non-EV)
Transformers Capacity	162.53 MVA	Total installed capacity

The model represents the 22 kV network with 91 buses and 102 lines. The total non-EV base load is 177.01 MW and 141.61 Mvar. All simulations use a 400 MVA base. Units were harmonized, graph connectivity verified, and per-unit voltage limits set to 0.95 – 1.05. A complete description of input field names and units is provided in the Appendix.

Spatial Proxy for Public Charging Sites

In the absence of a finalized siting plan, fuel-retail locations (gas stations) are used as proposed public charging sites. Public-session energy is mapped to the nearest site (great-circle distance), preserving corridor clustering.

Home and Work Charging Attachment

Home/work charging attaches to the nearest load buses via proximity and basic land-use/population weights. When polygonal land-use data are coarse or missing, Euclidean proximity is used as a fallback, yielding bus-level weights for the home/work fractions.

Data Pre-Processing and Validation

Coordinate harmonization (WGS84), connectivity checks, rating/limit defaults (0.95–1.05 per unit), and base-load reconciliation to substation meters within **±5%** *(set to your actual value if different)* were performed. Cleaned tables (buses, branches, loads, stations) are versioned and used as the single source of truth.

Stochastic EV Load Profiling and Assumptions

Hourly EV demand is generated using a Monte Carlo model that specifies fleet composition, SoC/energy requirements, hour-of-day and seasonal shaping, charger selection, spatial mapping to buses, and exported artefacts.

Vehicle Classes and Parameters

Three fleets capture Oujda's transport modes **Table 2**.

Daily charging probability p_{chg}: cars 0.20, motorcycles 0.90, buses 0.50. Location split $(w_{\mathrm{h}}, w_{\mathrm{w}}, w_{\mathrm{p}})$: **home 0.20, work 0.20, public 0.60**. Available charger powers: home **3.7 kW**; public **22/50/120 kW** (brand-dependent mix). EV demand is modelled at **unity power factor** unless stated otherwise.

Table 2. Vehicles characteristic

Vehicle Type	Quantity	Daily Distance [km]	Battery capacity [kWh]	Efficiency [kWh/km]
Cars	56 [%]	30	44	0.20
Motorcycles	26 [%]	30	1.56	0.05
Buses	18 [%]	210	324	1.50

This fleet mix was chosen specifically to reflect the unique transportation landscape of Oujda, where motorcycles and public buses represent a significant portion of urban mobility. A 'car-only' model, as seen in many European or US-based studies [26], would fail to capture this local reality, and our multi-vehicle approach provides a more realistic composite load profile.

Daily energy requirement and *SOC*

Daily energy per vehicle $Edaily_{\mathrm{v}}$:

$$Edaily_v = D_v \times \eta_v \; [kWh/day] \tag{1}$$

where D_{v} represents the daily distance traveled (for instance, in Morocco D_{car} = 30 [km]) [27] and η_{v} denotes the vehicle's energy efficiency, parameters derived from regional driving surveys and manufacturer specifications. Furthermore, the Python code simulates the state-of-charge *SOC* dynamics for each vehicle, determining the charging requirement based on battery capacity (C_{v}) and predefined thresholds. For example, a car with $C_{\mathrm{car}} = 44[\,\mathrm{kWh}]$ that needs to recharge from 30% to 80% *SOC* would require an energy input calculated as:

$$Echarge = C_{\mathrm{v}} \times (target\_SOC - initial\_SOC) \tag{2}$$

To introduce realism, stochasticity is incorporated via probabilistic charging behavior, modeled as [28]:

$$\mathrm{ChargeToday}_v \sim \mathrm{Bernoulli}(p_v) \tag{3}$$

Hour-of-day shaping

Addressing temporal variability, the simulation further incorporates two essential mechanisms. First, it applies time-of-use weighting by assigning hourly charging probabilities

$P(h)$ based on normalized weights w_{h} which capture peak and off-peak charging preferences (for instance, higher weights for overnight residential charging):

$$P(h) = \frac{w_h}{\sum_{i=1}^{24} w_i} \tag{4}$$

Evening-dominant kernel (urban after-work arrivals): 18–23 → **8**; 06–08 → **2**; other hours → **1**. (This corrects the earlier inversion and matches the observed evening peak.)

Seasonality

Monthly multipliers α_{s} adjust EV energy for HVAC and thermal-management overheads (eq. (5)). Values are bounded in **[0.95, 1.10]** (temperate–hot climates). **Table 3** lists the factors used.

$$E^{\text{seasonal}} = E_{\mathrm{v}}^{\text{daily}} \times \alpha_{\mathrm{s}} \tag{5}$$

Table 3.Monthly seasonality factors α_s

Month	Jan	Feb	Mar	Apr	May	Jun	Jul	Aug	Sep	Oct	Nov	Dec
α factor	1.10	1.00	1.00	1.00	0.95	1.05	1.10	1.10	1.00	1.00	1.05	1.10

Nominal values: winter 1.05; shoulder (Mar – May; Oct – Nov) 1.00; summer 0.95.

Charger Assignment and Power Limits

At the selected node, a charger type is drawn (home 3.7 kW; public 22/50/120 kW). Session power is bounded by the charger rating, and cumulative session energy is capped to deliver $\alpha_{\mathrm{s}} E_{\text{charge}}$. Hourly resolution ($\Delta t = 1$ h)is used; the final hour may be partial:

$$0 \le P_i(t) \le P_{charger}^{max}, \sum_{h \in session} P_i(h)\, \Delta t \le \alpha_s\, E^{charge} (\Delta t = 1\ h) \tag{6}$$

Session duration equals the smallest integer hours satisfying energy delivery; partial final-hour energy is allowed.

Spatial Allocation to Buses

If a session occurs, location $\ell \in \{\text{home}, \text{work}, \text{public}\}$ is drawn with probabilities $(w_{\mathrm{h}}, w_{\mathrm{w}}, w_{\mathrm{p}})$. Public sessions map to the nearest station and then to its serving bus; home/work map to the nearest load bus (proximity/land-use weights). Summation over sessions mapped to bus b yields hourly EV demand $L_{\mathrm{EV}}(t, b)$.

Monte-Carlo Sampling and Artefacts

Each scenario is simulated for 8,760 h. A single run draws $\{D_i\}$, daily charging decisions, locations, and start times; optional uncertainty uses multiple seeds to summarize median and 5–95% bands. For each scenario/seed, exported artefacts include: (i) $L_{\mathrm{EV}}(t,b)$; (ii) bus-level net loads; and (iii) station/session summaries (counts, energy, mean session length).

Load Profile Generation

A full-year, seasonal Monte Carlo simulation produces the high-resolution electric-vehicle load $L_{\mathrm{EV}}(t,b)$for each scenario; this file is the primary artefact of the demand model.

Penetration Scenarios

Three adoption levels are assessed: 0% (no EV), 10%, and 30%.To ensure policy relevance, the 10% and 30% penetration scenarios were grounded in national-level adoption forecasts for Morocco. Projections from a 2019 technical report on sustainable mobility by Morocco's Energy Federation [29] outline several adoption pathways. Our scenarios are derived from these national-level forecasts, representing conservative and ambitious bounds.

Net Nodal Demand for Steady-State Analysis

This study uses a single steady-state snapshot for the grid impact assessment. To create the input for this grid model, we first calculate the annual average EV power $L_{\mathrm{EV,avg}}(b)$ for each bus from the 8760-hour load profile generated by Model 1.

The total load for each bus $L_{\mathrm{total}}(b)$ is then calculated by superposing this annual average EV power onto the base network load $L_{\mathrm{base}}(b)$:

$$L_{total}(b) = L_{base}(b) + L_{ev,ave}(b) \tag{7}$$

Power-Flow Solution

A single steady-state power flow is solved for each scenario using GridCal and the net nodal demands above:

- **Algorithm:** alternating-current Newton–Raphson
- **Tolerance:** 1×10^{-6}per unit; **maximum iterations:** 25
- **Slack bus:** primary supply node at the 225/60/22 kV interface
- **Load models:** base loads as *P*–*Q*; EV charging at unity power factor
- **Operating limits:** bus voltages checked against **0.95–1.05 per unit**; branches/transformers flagged above **100%** of S_{rate}

Line-Loading Definition

Line/transformer loading uses apparent power (active $P_{\mathrm{line}}$and reactive Q_{line}) normalized by the nameplate rating S_{rate}, [30], [31]:

$$\text{Loading } [\%] = \frac{\sqrt{P_{\mathrm{line}}^2 + Q_{\mathrm{line}}^2}}{S_{\mathrm{rate}}} \times 100 \tag{8}$$

Stress Metrics for Steady-State Analysis

This subsection defines the indicators computed from each single steady-state snapshot (0%, 10%, 30%) and how they are used to compare performance across adoption levels.

- **Voltage quality**
  - Record bus voltages (per unit) on all energized buses.
  - Report the minimum bus voltage in the network.
  - Count buses below the 0.95 per unit planning limit (and optionally below 0.90 per unit).
- **Thermal Loading**
  - Record line and transformer loading as a percentage of nameplate rating.
  - Report the maximum element loading in the network.
  - Tabulate shares of elements within the bands: ≤70%, 70 – 90%, 90 – 100%, and >100% (overloaded).
- **Substation electric-vehicle energy shares**
  - Aggregate **electric-vehicle (EV)** average charging power to the supplying primary substation.
  - Report the spatial distribution of this EV load to identify substations that receive the largest shares (“hotspots”).

RESULTS

This section presents the first-week unmanaged charging behavior at two adoption levels. **Figure 2a**, **Figure 2b**, **Figure 2c** and **Figure 2d** illustrate disaggregation by location and system aggregation for 10% and 30% EV penetration. Location-specific views (**Figure 2a**, **Figure 2c**) show that public sites generate the largest intermittent spikes, while home and work sessions are smaller but frequent. System-level views (**Figure 2b**, **Figure 2d**) reveal a pronounced evening shoulder (~18:00 – 23:00) and a smaller mid-day shoulder. Between 10% and 30% adoption, the evening peak increases more than proportionally, reflecting nonlinear growth driven by coincident starts at public sites.

Snapshot Power-Flow Convergence

Solver performance for the steady-state snapshots is reported here. Using annual-average charging injections, a single alternating-current Newton – Raphson solve was executed for each scenario (0%, 10%, 30%) with a mismatch tolerance of 1×10^{-6}. All cases converged cleanly, with final residuals well below tolerance: 0%: 9.11×10^{-11} p.u.; 10%: 3.36×10^{-6} p.u.; 30%: 9.58×10^{-11} p.u. Computation time was negligible.

Charging Distribution Across Substations

Figure 3 displays the EV-only average charging power (excluding base load) mapped to the nearest primary substation for 10% and 30% adoption. The distribution is non-uniform: several corridors absorb disproportionate shares. The increase from 10% to 30% is not proportional across substations, as proposed public charging sites (gas stations) act as spatial proxies, concentrating sessions where site density is higher.

Figure 2. (a) Charging power by location—10% adoption (Home, Work, Public); (b) Total system EV-charging power—10% adoption; (c) Charging power by location—30% adoption (Home, Work, Public); (d) Total system EV-charging power—30% adoption

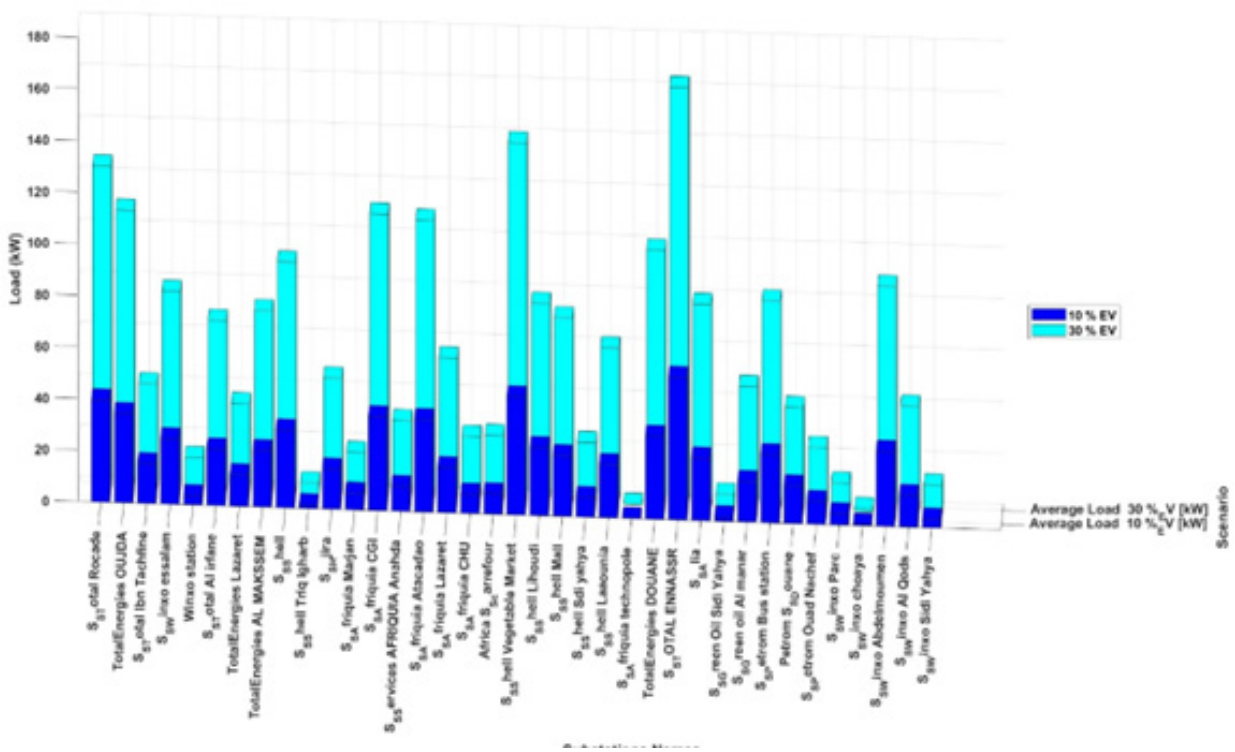

Figure 3. Average Load Distribution Across EV Charging Stations at Different Utilization Levels (10%, 30%)

Network-Wide Loading Patterns

Figure 4a – 4c presents branch loading across the network for 0%, 10%, and 30% scenarios, using the study bands: ≤70% (green), 70 – 90% (yellow), 90 – 100% (orange), and >100% (red). As adoption rises, yellow/orange/red segments expand along corridors with multiple proposed sites, indicating spatial clustering of stress. For illustration, Line_Autohall – Oujda – Omran3 increases from ~73% (baseline) to ~86% (10%) and ~96% (30%).

Thermal headroom remains concentrated in the ≤70% band, but a discernible tail moves into higher bands as EV adoption increases, thermal stress intensifies modestly across the network. At baseline (0% EV), 78.6% of lines operate at ≤70% of their thermal rating, 9.4% fall within the 70 – 90% band, 3.4% within 90 – 100%, and 6% exceed 100%. At 10% EV penetration, these shares shift to 76.9%, 10.3%, 5.4%, and 7%, respectively. At 30% EV, the distribution becomes 75.2%, 10.4%, 6.3%, and 9%. The largest increases occur on feeders serving corridors with multiple proposed public-charging sites, consistent with the spatial clustering illustrated in **Figure 4** and quantified in **Figure 5**.

This subsection summarizes voltage quality at energized buses. **Figure 6**. eports per-bus voltage drop $(1 - V)$for the 0%, 10%, and 30% snapshots. The distribution is concentrated at small drops: 94 of 103 buses (≈91%) exhibit ≤3% drop in all scenarios, while a narrow, persistent tail of 7/103 lies >10%, co-located with charging hotspots. In per-unit terms, the system bulk is stable (median voltage ≈ 0.974 p.u. across scenarios). Relative to planning thresholds, about 9 buses fall below 0.95 p.u., and none fall below 0.90 p.u.; these counts change little with adoption.

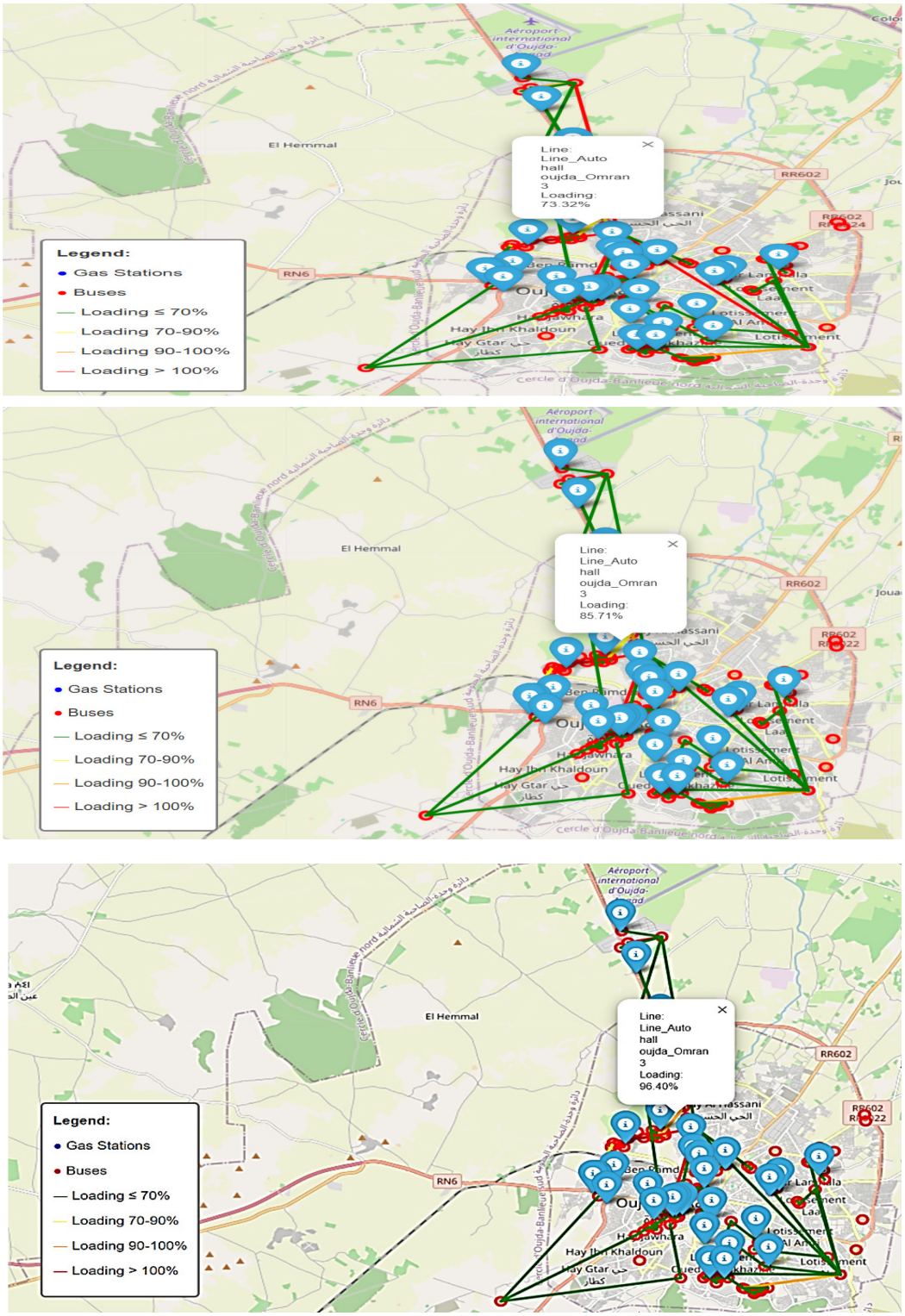

Figure 4.Comparative Visualization of Urban Grid Loading under Different EV Penetration Scenarios (0%, 10%, and 30%) is depicted as: **Figure 4a** (a); **Figure 4b** (b); and **Figure 4c** (c)

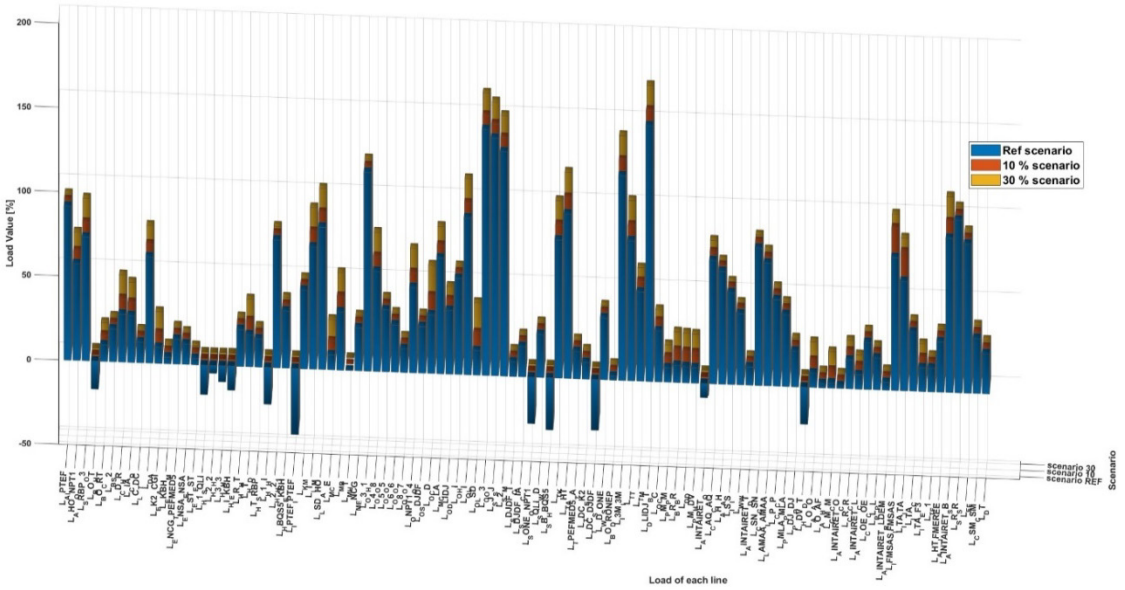

Figure 5. Loading Percentage Across Different Lines at Various Utilization Levels (0[%], 10[%], 30[%])

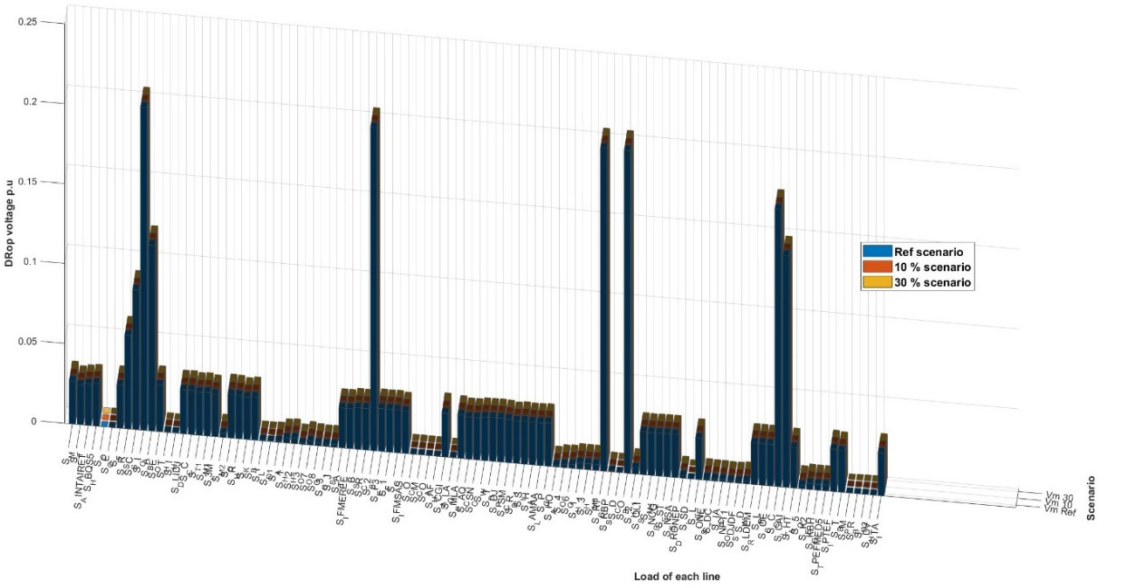

Figure 6. Voltage Drop Profiles Across Substations under Varying EV Penetration

DISCUSSION

The results show a clear pattern: broad system headroom with localized, pre-existing stress that is amplified by EV adoption. The finding that the grid is "robust in bulk" (81% of lines <70% loaded) but has a "weak tail" (6% overloads, 9 undervoltage buses) is a key, nuanced outcome. This confirms that unmanaged charging does not push the entire system to collapse, but rather intensifies stress at known bottlenecks. This is a direct result of the non-proportional, spatial clustering of EV load (**Figure 3**).

This operating picture argues against system-wide reinforcement. With ~80% of branches lightly loaded, uniform upgrades would be low-yield. Instead, targeted levers are justified: (i) Selective reinforcement at the handful of "hotspot" feeders; (ii) Siting guidance for public chargers to avoid already-stressed corridors; and (iii) Simple operational measures (e.g., power caps), which are an important first step for mitigation.

This study deliberately used a steady-state assessment for its screening value: it is fast, reproducible, and transparent for planners in data-scarce systems. This "Limitations" section addresses all remaining analytical points:

- The analysis uses snapshots and does not capture worst-hour coincidence peaks, which are likely higher. Results are a conservative baseline.
- We did not simulate coordinated charging or bidirectional (V2G) support, which are both key areas for future work.
- Spatial and behavioral data are proxies, as local Moroccan telemetry is not yet available.
- Harmonics and non-unity power factors are excluded.

Even with these limits, the qualitative picture is robust: medians stay stable while the same corridors dominate the "weak tail." For research, the natural extension is a time-series analysis to test the mitigation and V2G strategies on the specific hotspots identified in this paper.

CONCLUSIONS

We evaluated unmanaged electric-vehicle charging impacts on a medium-voltage distribution network representative of Oujda using a reproducible, geo-referenced steady-state workflow. Despite rising adoption, network-wide headroom remains substantial – with 81%, 79%, and 78% of lines at ≤70% of rating across the 0%, 10%, 30% scenarios – and voltage quality is robust in bulk (≈91% of buses within ≤3% drop; median ≈ 0.974 p.u.; no bus below 0.90 p.u.). Stress manifests as a localized tail: the share of overloaded lines (>100%) grows modestly (6% → 7% → 9%), and a stable set of 7/103 buses exhibits >10% drop near public-charging hotspots.

These results argue for targeted interventions rather than uniform upgrades. Practical next steps for planners include: (i) selective reinforcement at a handful of hotspot feeders; (ii) siting guidance for public chargers to avoid already-stressed corridors; and (iii) simple operational measures during the evening shoulder (e.g., caps or staggered starts at fast chargers).

Future work should extend this baseline by quantitatively testing mitigation – coordinated charging policies, evening demand caps, and, where feasible, bidirectional vehicle-to-grid – and by coupling distributed solar and storage to absorb mid-day energy and reduce evening coincidence. A fuller time-series analysis with thermal time constants and feeder-level measurements would strengthen validation, but the present snapshots already provide actionable screening for hosting capacity in data-constrained settings.

ACKNOWLEDGMENT

The authors express their gratitude for the support received from the CNRST under the «PhD-Associate Scholarship-Pass» Program.

The paper is prepared within the framework of the EMERGE project, Call for proposals: HORIZON-CL5-2022-D3-02. Project number: 101118278. Type of action: Research and innovation actions HORIZON, 2023

NOMENCLATURE

C_v	battery capacity of the vehicle	[kWh]
D_v	daily distance traveled by the vehicle	[km]
$E_{v,t}$	energy consumption of the vehicle at time t	[kWh]
$P_{charging}$	charging power of the vehicle	[kW]
$P(h)$	hourly charging probability	[-]
P_{line}	active power flowing through a transmission line	[kW]
Q_{line}	reactive power flowing through a transmission line	[kVar]
SOC	state of charge of the battery	[%]
SOC_{final}	final state of charge of the battery	[%]
$SOC_{initial}$	initial state of charge of the battery	[%]
w_h	normalized weight for home charging share	[-]
w_w	normalized weight for workplace charging share	[-]
w_p	normalized weight for public charging share	[-]

Greek Letters

α_s	seasonal adjustment factor for energy demand	[-]
η_v	energy efficiency of the vehicle	[kWh/km]

Subscripts and Superscripts

max	maximum value
min	minimum value
v	refers to a specific vehicle
t	refers to a specific time step

Abbreviations

EV	Electric Vehicle
GridCal	Grid Calculation Software
PV	Photovoltaic
API	Application Programming Interface
IEA	International Energy Agency
NDC	Nationally Determined Contribution
TOU	Time of Use

REFERENCES

1. I. Energy Agency, "Global EV Outlook 2021 Accelerating ambitions despite the pandemic," 2021, https://iea.blob.core.windows.net/assets/ed5f4484-f556-4110-8c5c-4ede8bcba637/GlobalEVOutlook2021.pdf, [Accessed: Nov. 26, 2025].
2. F. Jelti, A. Allouhi, S. G. Al-Ghamdi, R. Saadani, A. Jamil, and M. Rahmoune, "Environmental life cycle assessment of alternative fuels for city buses: A case study in Oujda city, Morocco," *Int J Hydrogen Energy*, vol. 46, no. 49, pp. 25308–25319, Jul. 2021, https://doi.org/10.1016/J.IJHYDENE.2021.05.024.
3. J. Terrapon-Pfaff and S. Amroune, "Implementation of Nationally Determined Contributions - Morocco," 2025, https://newclimate.org/sites/default/files/2022-04/2018-11-30_climate-change_30-2018_country-report-morocco.pdf, [Accessed: Nov. 26].
4. MICHAËL TANCHUM, "MOROCCO'S GREEN MOBILITY REVOLUTION: THE GEO-ECONOMIC FACTORS DRIVING ITS RISE AS AN ELECTRIC VEHICLE MANUFACTURING HUB," 2022, https://www.mei.edu/sites/default/files/2022-08/Tanchum%20-%20Morocco%20Green%20Mobility%20Revolution.pdf, [Accessed: Nov. 01, 2025].
5. Y. Rhannouch, A. Saadaoui, and A. Gaga, "Analysis of the impacts of electric vehicle chargers on a medium voltage distribution network in Casablanca City," *e-Prime - Advances in Electrical Engineering, Electronics and Energy*, vol. 11, p. 100879, Mar. 2025, https://doi.org/10.1016/J.PRIME.2024.100879.
6. V. Umoh, A. Adebiyi, and K. Moloi, "Hosting Capacity Assessment of South African Residential Low-Voltage Networks for Electric Vehicle Charging," *Eng 2023, Vol. 4, Pages 1965-1980*, vol. 4, no. 3, pp. 1965–1980, Jul. 2023, https://doi.org/10.3390/ENG4030111.
7. B. B. Gicha, L. T. Tufa, and J. Lee, "The electric vehicle revolution in Sub-Saharan Africa: Trends, challenges, and opportunities," *Energy Strategy Reviews*, vol. 53, p. 101384, May 2024, https://doi.org/10.1016/J.ESR.2024.101384.
8. G. A. Putrus, P. Suwanapingkarl, D. Johnston, E. C. Bentley, and M. Narayana, "Impact of electric vehicles on power distribution networks," in *2009 IEEE Vehicle Power and Propulsion Conference (VPPC)*, 2009, pp. 827–831, https://doi.org/10.1109/VPPC.2009.5289760.
9. J. A. P. Lopes, F. J. Soares, and P. M. R. Almeida, "Integration of Electric Vehicles in the Electric Power System," *Proceedings of the IEEE*, vol. 99, no. 1, pp. 168–183, 2011, https://doi.org/10.1109/JPROC.2010.2066250.
10. K. Clement-Nyns, E. Haesen, and J. Driesen, "The impact of vehicle-to-grid on the distribution grid," *Electric Power Systems Research*, vol. 81, no. 1, pp. 185–192, 2011, https://doi.org/10.1016/j.epsr.2010.08.007.
11. A. Dubey and S. Santoso, "Electric Vehicle Charging on Residential Distribution Systems: Impacts and Mitigations," *IEEE Access*, vol. 3. Institute of Electrical and Electronics Engineers Inc., pp. 1871–1893, 2015, https://doi.org/10.1109/ACCESS.2015.2476996.
12. J. Sarda, N. Patel, H. Patel, R. Vaghela, B. Brahma, A. K. Bhoi, and P. Barsocchi, "A review of the electric vehicle charging technology, impact on grid integration, policy consequences, challenges and future trends," *Energy Reports*, vol. 12, pp. 5671–5692, 2024, https://doi.org/10.1016/j.egyr.2024.11.047.
13. O. Sundstrom and C. Binding, "Flexible Charging Optimization for Electric Vehicles Considering Distribution Grid Constraints," *IEEE Trans Smart Grid*, vol. 3, no. 1, pp. 26–37, 2012, https://doi.org/10.1109/TSG.2011.2168431.

14. A. Emadi, Y. Lee, and K. Rajashekara, "Power Electronics and Motor Drives in Electric, Hybrid Electric, and Plug-In Hybrid Electric Vehicles," *Industrial Electronics, IEEE Transactions on*, vol. 55, pp. 2237–2245, 2008, https://doi.org/10.1109/TIE.2008.922768.
15. L. Gan, U. Topcu, and S. Low, "Optimal decentralized protocol for electric vehicle charging," *IEEE Transactions on Power Systems*, vol. 28, pp. 940–951, 2013, https://doi.org/10.1109/TPWRS.2012.2210288.
16. N. I. Nimalsiri, E. L. Ratnam, C. P. Mediwaththe, D. B. Smith, and S. K. Halgamuge, "Coordinated charging and discharging control of electric vehicles to manage supply voltages in distribution networks: Assessing the customer benefit," *Appl Energy*, vol. 291, p. 116857, Jun. 2021, https://doi.org/10.1016/J.APENERGY.2021.116857.
17. B. K. Sovacool, J. Kester, L. Noel, and G. Zarazua de Rubens, "Actors, business models, and innovation activity systems for vehicle-to-grid (V2G) technology: A comprehensive review," *Renewable and Sustainable Energy Reviews*, vol. 131, p. 109963, Oct. 2020, https://doi.org/10.1016/J.RSER.2020.109963.
18. P. Kumar, H. K. Channi, R. Kumar, A. Rajiv, B. Kumari, G. Singh, S. Singh, I. F. Dyab, and J. Lozanović, "A comprehensive review of vehicle-to-grid integration in electric vehicles: Powering the future," *Energy Conversion and Management: X*, vol. 25, p. 100864, Jan. 2025, https://doi.org/10.1016/J.ECMX.2024.100864.
19. M. S. Mastoi, S. Zhuang, H. M. Munir, M. Haris, M. Hassan, M. Alqarni, and B. Alamri, "A study of charging-dispatch strategies and vehicle-to-grid technologies for electric vehicles in distribution networks," *Energy Reports*, vol. 9, pp. 1777–1806, Dec. 2023, https://doi.org/10.1016/J.EGYR.2022.12.139.
20. F. Alfaverh, M. Denaï, and Y. Sun, "Optimal vehicle-to-grid control for supplementary frequency regulation using deep reinforcement learning," *Electric Power Systems Research*, vol. 214, p. 108949, Jan. 2023, https://doi.org/10.1016/J.EPSR.2022.108949.
21. P. Richardson, D. Flynn, and A. Keane, "Optimal Charging of Electric Vehicles in Low-Voltage Distribution Systems," *IEEE Transactions on Power Systems*, vol. 27, no. 1, pp. 268–279, 2012, https://doi.org/10.1109/TPWRS.2011.2158247.
22. Y. Mu, J. Wu, N. Jenkins, H. Jia, and C. Wang, "A Spatial–Temporal model for grid impact analysis of plug-in electric vehicles," *Appl Energy*, vol. 114, pp. 456–465, 2014, https://doi.org/10.1016/j.apenergy.2013.10.006.
23. "GitHub - SanPen/GridCal: GridCal, a cross-platform power systems software written in Python with user interface, used in academia and industry," https://github.com/SanPen/GridCal, [Accessed: Aug. 01, 2025].
24. S. Blechmann, I. Sowa, M. H. Schraven, R. Streblow, D. Müller, and A. Monti, "Open source platform application for smart building and smart grid controls," *Autom Constr*, vol. 145, p. 104622, Jan. 2023, https://doi.org/10.1016/J.AUTCON.2022.104622.
25. R. D. Zimmerman, C. E. Murillo-Sanchez, and R. J. Thomas, "MATPOWER: Steady-State Operations, Planning, and Analysis Tools for Power Systems Research and Education," *IEEE Transactions on Power Systems*, vol. 26, no. 1, pp. 12–19, 2011, https://doi.org/10.1109/TPWRS.2010.2051168.
26. H.- Rivera, L. Hernandez, A. C.; Irizarry-Rivera, A. Huaman-Rivera, R. Calloquispe-Huallpa, A. C. Luna Hernandez, and A. Irizarry-Rivera, "An Overview of Electric Vehicle Load Modeling Strategies for Grid Integration Studies," *Electronics 2024, Vol. 13, Page 2259*, vol. 13, no. 12, p. 2259, Jun. 2024, https://doi.org/10.3390/ELECTRONICS13122259.

27. A. Chachdi, B. Rahmouni, and G. Aniba, "Socio-economic Analysis of Electric Vehicles in Morocco," *Energy Procedia*, vol. 141, pp. 644–653, 2017, https://doi.org/10.1016/j.egypro.2017.11.087.
28. S. Sinharay, "Discrete Probability Distributions," in *International Encyclopedia of Education (Third Edition)*, P. Peterson, E. Baker, and B. McGaw, Eds. Oxford: Elsevier, 2010, pp. 132–134.
29. Fédération de l'Énergie, "Study on Sustainable Mobility in Morocco" (In French : Etude sur la mobilité durable au Maroc)," https://www.fedenerg.ma/wp-content/uploads/2019/07/Federation-de-lEnergie-Etude-sur-la-Mobilite-Durable-au-Maroc-Version-Complete-Juin-2019.pdf, [Accessed: Nov. 01, 2025].
30. S. B. Crary, "Transmission-line electric loadings," *Electrical Engineering*, vol. 63, no. 12, pp. 1198–1204, Jul. 2013, https://doi.org/10.1109/EE.1944.6440668.
31. J. D. Glover, T. J. Overbye, and M. S. Sarma, *POWER SYSTEM ANALYSIS & DESIGN*. Boston, USA: Cengage Learning, 2017.

APPENDIX

Table A1. Bus parameters

Parameter	Description
name	Unique identifier for the bus (e.g., substation name)
V_{nom}	Nominal operating voltage (kV)
V_{min}	Minimum voltage limit (p.u.)
V_{max}	Maximum voltage limit (p.u.)
longitude	Geospatial coordinate for mapping
latitude	Geospatial coordinate for mapping

Table A2. Branch parameters

Parameter	Description
name	Unique identifier for the line
bus_from	Name of the sending-end bus
bus_to	Name of the receiving-end bus
R	Line resistance (p.u. or Ohms)
X	Line reactance (p.u. or Ohms)
B	Line susceptance (p.u. or S)
length	Physical length of the line (km)
Parameter	Description
name	Unique identifier for the load
bus	Name of the bus the load is connected to
P	Base active power demand (MW)
Q	Base reactive power demand (Mvar)

Table A3. Transformer types

Capacity (kVA)	Count (Units)	Total Capacity (MVA)
50	1	0.05
100	5	0.50
160	15	2.40
200	2	0.40
250	21	5.25
315	12	3.78
400	41	18.00
500	6	3.00
630	10	9.45
800	4	3.20
1000	2	2.00
40,000 (40 MVA)	4	160.00

Paper submitted: 01.08.2025
Paper revised: 19.12.2025
Paper accepted: 03.01.2026